Nonlinear Dyn (2010) 61: 83–99
DOI 10.1007/s11071-009-9633-6

ORIGINAL PAPER

Comparison of seismic performance of three restrainers for multiple-span bridges using fragility analysis

E. Choi · J. Park · S.-J. Yoon · D.-H. Choi · C. Park

Received: 25 November 2008 / Accepted: 26 November 2009 / Published online: 9 December 2009

Abstract Steel restrainer cables for multiple-frame bridges in California in the United States showed the effectiveness to prevent the unseating at the internal hinges during the past several earthquakes. After that, the steel restrainer cables are being tried to apply for multiple-span-simply-supported (MSSS) bridges in the central and the southeastern regions in the United States. In addition, shape memory alloy (SMA) bars in tension are being studied for the same application. In multiple-frame bridges, the developed seismic forces are transferred to piers through the restrainers; however, in MSSS bridges, the seismic forces are transferred to abutments by the restrainers. Therefore, the abutment's behavior should be investigated as well. This study assesses the seismic performance of the three types of restrainers—steel restrainer cables, SMA bars in tension, and SMA bars in bending for MSSS bridges—due to moderate to strong ground motions using a deterministic seismic analysis. Also, a fragility analysis is conduced to assess the seismic resistance for the overall bridge system. For these analyses, the bending test of an SMA bar is conducted and its analytical model is determined. Then, nonlinear time history analyses are conducted to assess the seismic responses of the as-built and the retrofitted bridges. The deterministic analysis illustrates how the restrainers influence the components of the bridge. However, it could not explain the effects on the whole bridge system. The fragility analysis shows the effects of the three restrainers on the overall bridge system. The fragility analysis indicates that the SMA bars in bending are the most effective ones.

Keywords Shape memory alloy · Restrainer · Unseating · MSSS bridges · Abutments

E. Choi (✉) · S.-J. Yoon
Department of Civil Engineering, Hongik University, Seoul 121-791, Korea
e-mail: eunsoochoi@hongik.ac.kr

J. Park
Railroad Structure Research Department, Korea Railroad Research Institute, Uiwang 437-757, Korea

D.-H. Choi
Department of Civil and Environmental Engineering, Hanyang University, Seoul 133-791, Korea

C. Park
Department of Civil Engineering, Kangwon National University, Samcheok 245-711, Korea

1 Introduction

The 1971 San Fernando earthquake resulted in the collapse of a larger number of bridges due to the unseating at hinge supports [1]. After that, California Department of Transportation (Caltrans) introduced steel restrainer cables (SRC) to protect bridges from the unseating [2], and the steel restrainer cables showed adequate performance during the 1989 Loma Prieta and the 1994 Northridge earthquakes. Based on a good

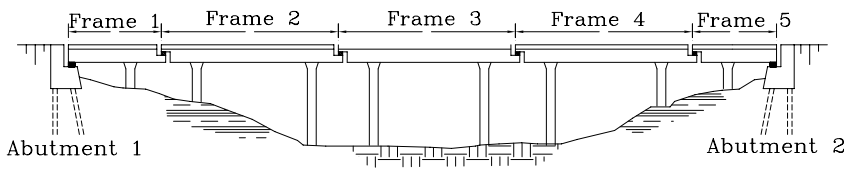

(a) Typical multiple-frame bridge

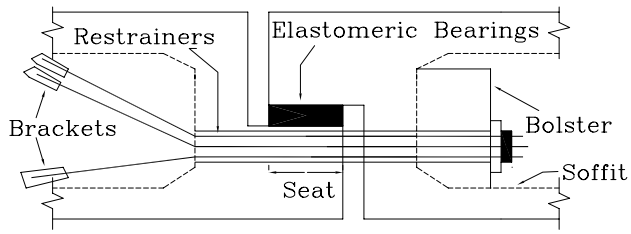

(b) Steel restrainer cable at internal hinge

Fig. 1 General view of a multiple-frame bridge and steel restrainer cable

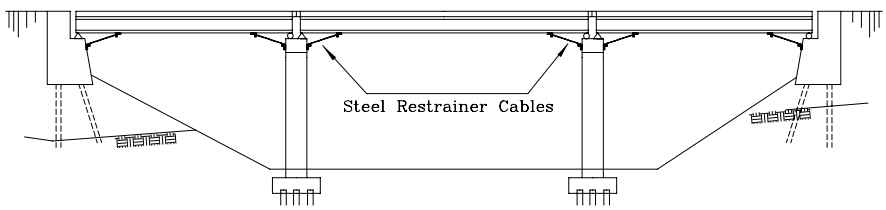

Fig. 2 Multiple-span-simple-supported bridge and installation of steel restrainer cables

performance of the steel restrainer cables in California, several studies made efforts to apply the steel restrainer cables for multiple-span-simply-supported (MSSS) bridges in Mid-America region, which includes several states in the southeastern and central United States. The typical type of bridges in California is the multiple-frame bridge in Fig. 1 which also shows the connection of the steel restrainer cables at internal hinges of the bridge. In the bridges, the developed seismic forces of the adjacent decks are transferred to piers through the cables. The cable-connection in the MSSS bridges, which are a typical type in the central and southeastern area, is in place at deck to abutment or deck to cap beam, as shown in Fig. 2. The developed forces in the bridges are transferred to the abutments via the cables. Therefore, in the MSSS bridges with the restrainers, differently from the multiple-frame bridges, the responses of bridge components including abutments should be investigated.

Shape memory alloy was introduced as a more effective restrainer for bridges than the steel restrainer cables. DesRoches and Delemont [3] conducted several tensile tests of superelastic SMA bars and wires and used the SMA bars in tension as restrainers for an MSSS bridge. They compared the results of the SMA bars in tension and the SRC and indicated the effectiveness of the SMA bars in tension to reduce the hinge opening. However, they did not check the influence on the abutments due to the restrainers during a ground motion shaking. The employment of the restrainers should guarantee that all the components of the bridge are not damaged seriously, and then, the practical applicability of the restrainers can be ensured.

There were a large number of studies on the seismic applications of SMA bars or wires in tension, compression, or both. However, the studies related to the application of SMAs in bending are rare for structures. Dolce et al. [4] used martensite and austenite SMA wires to develop a seismic damper having the self-centering capability and proved the effectiveness of the device through experimentations. Wilde et al. [5] used SMA bars placed with elastomeric

bearings for highway bridges. The system was validated analytically to reduce the relative deck displacement. DesRoches et al. [6] conducted the tensile tests of SMA bars and provided the mechanical behavior of the superelastic SMA bars. DesRoches and Delemont [3] and Andrawes and DesRoches [7] tested SMA tensile bar restrainers for MSSS and multiple-frame bridges, respectively. They addressed the effectiveness of the SMA tensile bars to restrain the relative deck displacements and their causes. However, Wilde indicated that SMA bars or plates are exposed to a buckling problem when they are used in compression. Also, SMA wires basically do not resist any compression. Therefore, it is difficult to use directional SMA bars properties under tension and compression. However, the bending of SMA bars may be used effectively as dampers or restrainers in both directions of pushing and pulling. Ocel et al. [8] used SMA bars subjected to bending to dissipate energy from the connection of beam and column in a steel frame. The bending application of SMAs for the bridge was Adachi's study [9]. He and his colleagues conducted the shaking-table tests of a reduced-scale bridge deck with SMA plates as an energy dissipater. Although Adachi used the bending behavior of SMA plates, he just provided the mechanical bending behavior of the plates indirectly. Choi et al. [10] recently provided the pure bending behavior of a superelastic SMA bar and showed its applicability for a seismic restrainer.

Recently, the fatigue of SMAs has become an important issue [11] since fatigue loading decreases the transformation stress and the energy dissipation capacity [12]. Bending rotation fatigue (BRF) is generally used as a standard test for the structural fatigue of shape memory alloy wires [13]. Wagner et al. [14] indicated that increasing rotational speed in a BRF test resulted in shorter rupture lives of NiTi shape memory wires while the wire was exposed to air. This was due to the increment of the SMAs' temperature according to the high speed loading. This result matched with that of Miyazaki et al.'s study [15]; they maintained that the high temperature of NiTi shape memory wires shortened their fatigue life.

In this study, three types of restrainers were investigated to assess their seismic performance for an MSSS bridge: the steel restrainer cables (SRC), the SMA bars in tension (SMA-T), and the SMA bars in bending (SMA-B). This study conducted several bending tests of an SMA bar and developed its analytical model as a restrainer.

2 Current methods for hinge opening problem

Unseating at internal hinges occurs when relative displacement between decks or deck and abutment exceeds the seat-width. The unseating in a bridge results in a total collapse and produces serious economic damages directly and indirectly. For a multiple-frame bridge in Fig. 1, the heights of columns for each frame are different in general and, thus, so are the fundamental periods of frames. An out-of-phase motion between frames due to the fundamental periods' difference may produce unseating. However, for the MSSS bridge in Fig. 2, the heights of columns are generally equal but the masses of decks are different. Thus, an out-of-motion between decks is possible. Also, during in-phase motion, the deck fixed to an abutment whose displacement is relatively very small may be unseated from the adjacent pier cap.

Several devices have been studied and applied for practical uses to prevent unseating, such as steel restrainer cables, seat extenders, viscous dampers, and metallic dampers. Padgett et al. addressed strong and weak points of several devices currently examined [16]. In addition, they showed the effectiveness of SMA bars in tension to restrain hinge openings for multiple-span bridges. Andrawes and DesRoches [7] conducted a similar study for multiple-frame bridges. The restrainer to prevent unseating can be categorized within two types: active in tension-only and active in both directions (pulling and pushing). Devices in tension-only are activated only with occurring opening. However, devices activated in both directions resist relative displacement with opening and closing. Steel restrainer cables and SMA bars in tension are typical devices in tension-only. Steel restrainer cables were being tried to apply for multiple-span bridges in Mid-America region (central and southeastern) after the success in California in the United States. Analytical and experimental studies have been conducted about the cables. SMA tensile bars were examined analytically for the effectiveness to limit openings at hinges and compared for the performance to other devices. Metallic and viscous dampers are the devices activated in both directions. Devices activated in both directions have a benefit to use the capacity of abutments in passive (pushing) direction in multiple-span bridges shown in Fig. 2. However, Padgget et al. [16] pointed out the drawbacks of these two devices. They maintained that metallic dampers whose behavior is

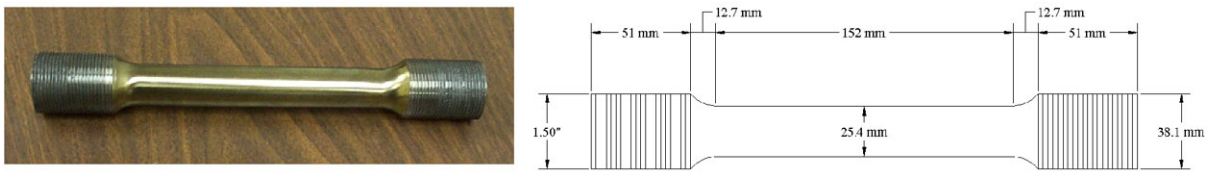

Fig. 3 Shape memory alloy superelastic bar tested

bilinear do not show adequate re-centering capacity, and that viscous dampers may transfer excessive forces to other parts of a bridge due to their velocity-dependant nature. Seat extenders are not categorized in the above two types since they do not transfer any force but provide additional seat-width that prevents unseating. They neither improve the relative displacement at hinges nor prevent the damage of other components.

3 Bending test of shape memory alloy bar

In the first phase of the study, an SMA bar was tested in bending. The 280 mm long and 25.4 mm in diameter Ni-44Ti (wt.%) SMA bar in Fig. 3 was used. The transformation temperatures of the specimen were measured by DSC (differential scanning calorimetry) shown in Fig. 4; A_s and A_f were -19.1 and 9.8°C, and M_s and M_f were -16.3 and -44.6°C, respectively. Thus, the specimen remains in austenitic state at room temperature above 9.8°C. Also, differently from the Kaounide's study [12], the specimen showed apparent superelastic behavior at room temperature and did not decrease the transformation stress during first several loading cycles [6].

To induce single curvature bending in the SMA bar, the top of the bar has to be fixed and a force at the bottom has to be applied perpendicular to the bar, as shown in Fig. 5. Also, the boundary condition at the bottom allows translational and rotational movement. For this purpose, a ball and a cylinder were specially manufactured, as shown in Fig. 6. Figure 5 shows the test setup, where the cylinder transferred a lateral force from the actuator to the ball which rotated freely inside the cylinder to allow the single curvature bending of the SMA bar. Also, Fig. 6 shows the jointed shape of a ball and the SMA bar and the deformed shape of the SMA bar. In the test setup, the ball did not touch the bottom of the cylinder and, thus, any compressive force did not apply on the SMA bar.

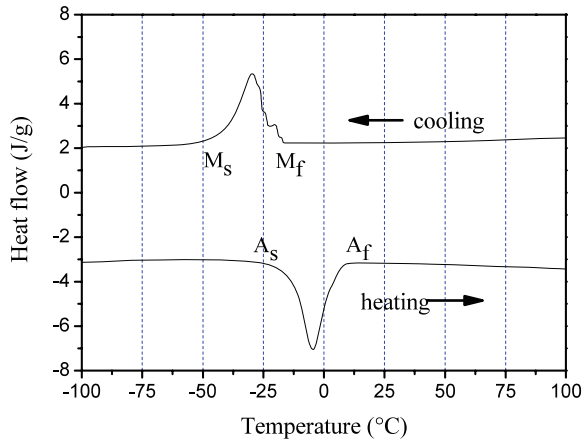

Fig. 4 DSC curve for the NiTi SMA specimen

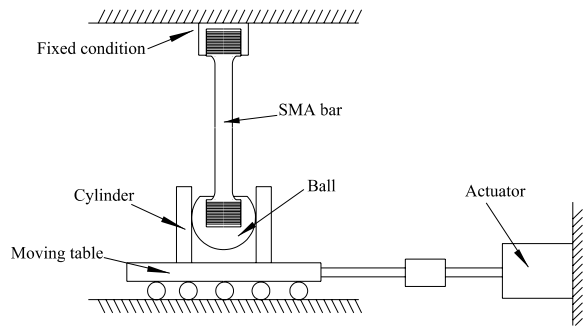

Fig. 5 Test setup for the single curvature bending of the SMA bar

The bending tests were performed under displacement control. The maximum displacements were varied from ±10 mm to ±40 mm with the increase of ±5 mm. The loading frequency was 0.025 Hz for quasi-static tests. For each displacement amplitude, three loading cycles were applied. The force–displacement curves of the SMA bar in bending are shown in Fig. 7. The loading paths almost did not vary with increasing maximum displacement, but the unloading paths became flat with large displacements.

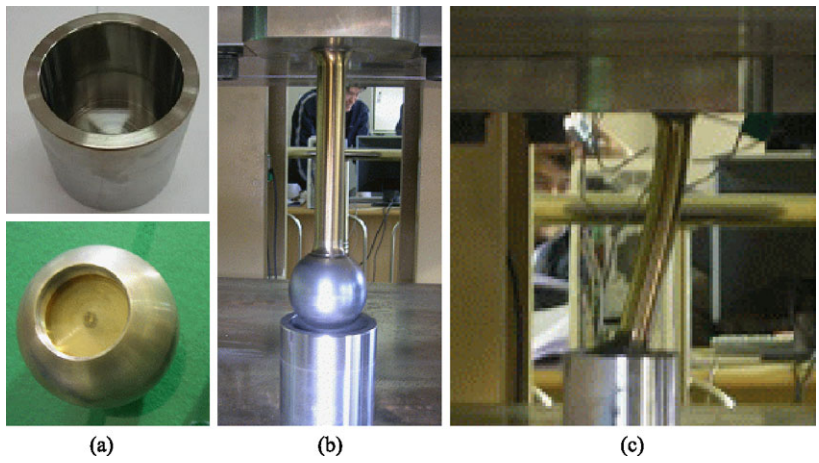

Fig. 6 Test setup for single bending; (**a**) a ball and a cylinder, (**b**) a ball bolted to the SMA bar and the cylinder welded at the bottom, (**c**) the shape of a single bending of the SMA bar

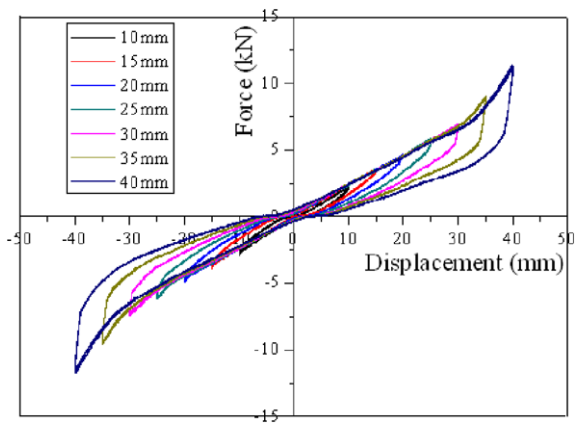

Fig. 7 Force–displacement curve from bending test of SMA bar

The average loading and the unloading stiffness were respectively 0.223 and 0.212 kN/mm.

4 Description and analytical modeling of the MSSS bridge

The bridge considered in this study consisted of three spans simply supported on multi-column bents, as shown in Fig. 8. Each span had 11 steel girders supported by steel bearings at the ends and each bent had four columns. The steel bearings were high-type rocker bearings for fixed and expansion conditions. The lengths of the side and the middle spans were 12.2 m and 24.4 m, respectively. The gaps between deck and abutment and between decks were 38.1 mm and 25.4 mm, respectively.

The bridge consisted of several components such as columns, abutments, steel bearings, foundations, superstructure, and pounding elements, exhibiting highly nonlinear behavior except for superstructure and foundations during an earthquake. Therefore, a two-dimensional nonlinear analytical model of the bridge in longitudinal direction was developed using DRAIN-2DX nonlinear analysis program [17]. The superstructure is usually expected to remain linear under longitudinal earthquake motions so that it could be modeled using a linear element. In the bridge model, the columns consisted of fiber elements for unconfined and confined concrete, and reinforcements. For each fiber, a stress–strain relationship describes the nonlinear behavior of each material. The steel bearings were modeled following the Mander's test [18]. The pile foundations were modeled with linear springs for horizontal and rotational directions considering the piles' capacity [19]. The impact element was used for pounding between the decks and between the deck and the abutment. The trilinear gap element in compression-only described the pounding break-out when the gap was closing.

The nonlinear abutment behavior in this study reflected the design recommendations from Caltrans and the experimental tests of abutments [2, 20]. As mentioned above, the characteristics of the abutments have a significant meaning since restrainers transfer large forces on them. The behaviors of the abutments for active and passive actions are shown in Fig. 9. The active action is according to the pulling action toward the deck and the passive action is according to the pushing action backward to the soil. The first yield in the active action occurred at 7.62 mm of 1619 kN and the

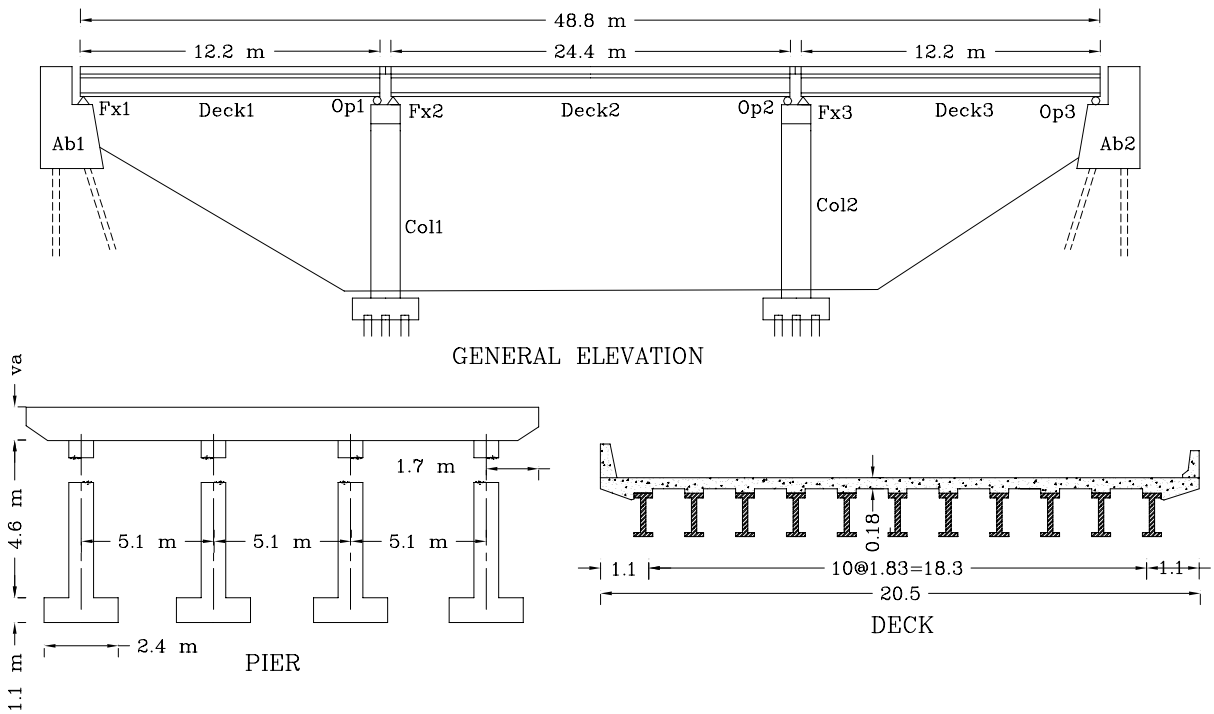

Fig. 8 General view of multi-span-simply-supported bridge with steel girders

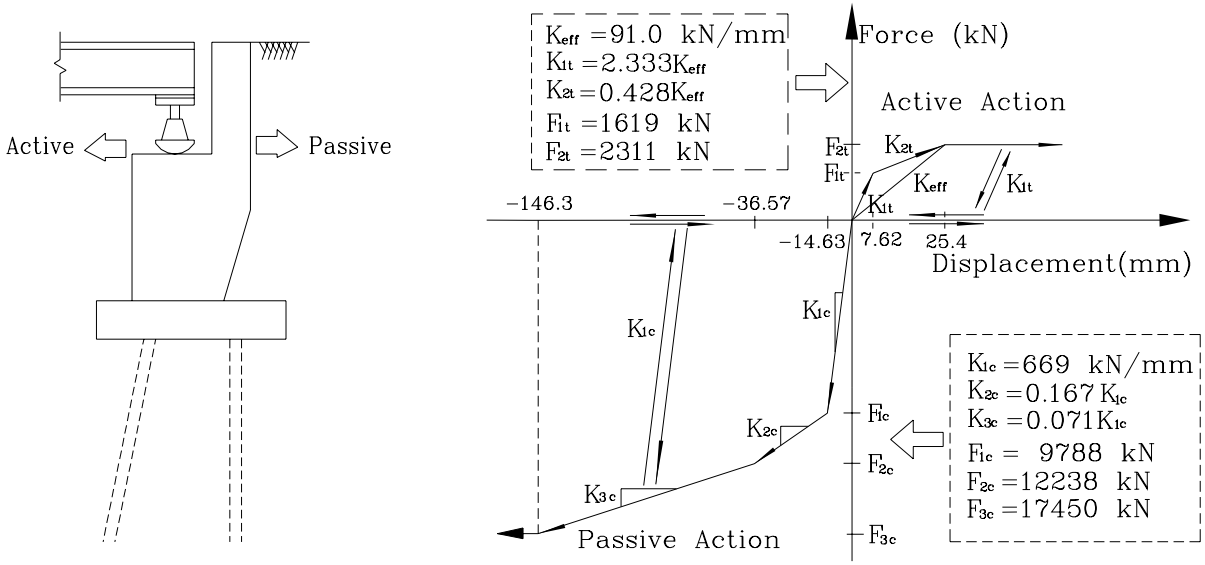

(a) Active and passive action

(b) Nonlinear behavior

Fig. 9 Nonlinear behavior of the abutments

ultimate strength was 2311 kN at 25.4 mm. In passive action, the first yield was developed at 14.63 mm of 9788 kN and the ultimate strength was 17450 kN at 146.3 mm. The initial stiffness was respectively 212 and 669 kN/mm for active and passive actions. The initial stiffness and the ultimate strength in the passive action were 3 and 7.5 times larger than those in the active action.

5 Analytical models and installation of restrainers

Based on the results of the experimental tests, an analytical model of the SMA bar in single bending was developed using a bilinear element. The initial and the post-yield stiffness were 2.16 and 0.216 kN/mm and the yield force was 0.5 kN. The analytical model is shown in Fig. 10 and it is compared to the experimental results. The analytical model accorded approximately with the experimental results but had almost the same loading stiffness as the experimental results.

The analytical model of the SMA in tension was based on the experimental tests, as shown in Fig. 11. The yield strength in loading path was 410 MPa at 1.5% strain and unloading yield strength was 138 MPa. Seven-percent strain hardening was applied up to 5% strain and 45% strain hardening was applied for a strain over 5%. The SMA bar in tension retained its residual deformation whose amount depends on the maximum strain. However, in the analytical model, the residual deformation was considered zero since the residual deformation was less than 1% with 5% strain deformation.

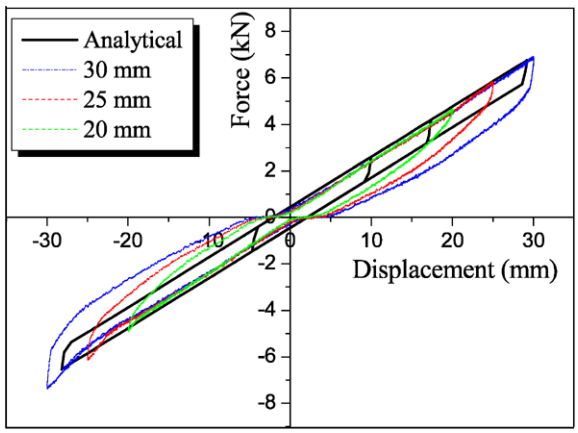

Fig. 10 Analytical model of the SMA bar in a single bending compared with experimental results

The assessed steel restrainer cables had the length of 1.52 m and the diameter of 19.1 mm, which had the yield strength of 174 kN at 30.5 mm. The cables were modeled as bilinear springs that resisted only to tension. The initial stiffness of the cables was 5.7 kN/mm and 5% hardening was assumed for the after-yield stiffness.

The SMA tensile bar evaluated was 0.61 m long to have the same tensile deformation of 30.5 mm at 5% strain and the diameter of the bar was the same as 19.1 mm of the steel restrainer cables. The initial stiffness of the SMA tensile bar was 12.83 kN/mm and the effective stiffness of the bar was 4.48 kN/mm up to 5% strain. Combining 20 SMA bending bars together, they had the effective stiffness of 4.6 kN/mm at 30.5 mm displacement. The properties of three restrainers are compared in Fig. 12. The steel restrainer

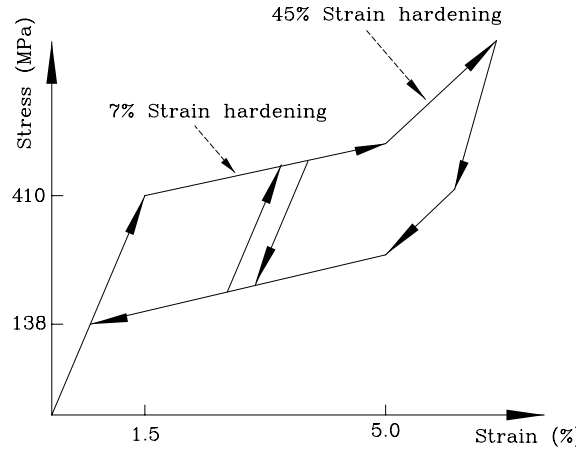

Fig. 11 Analytical model of SMA bar in tension

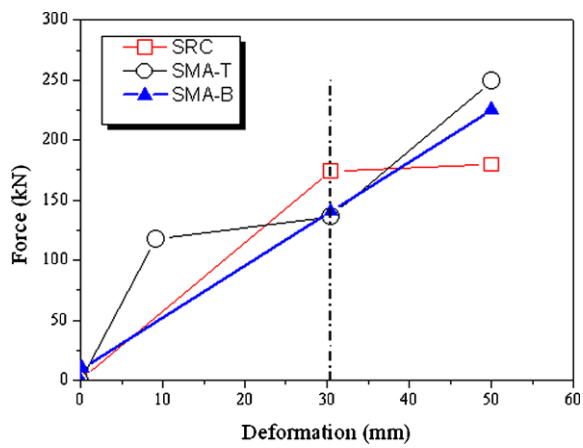

Fig. 12 Comparison of the three restrainers' behavior

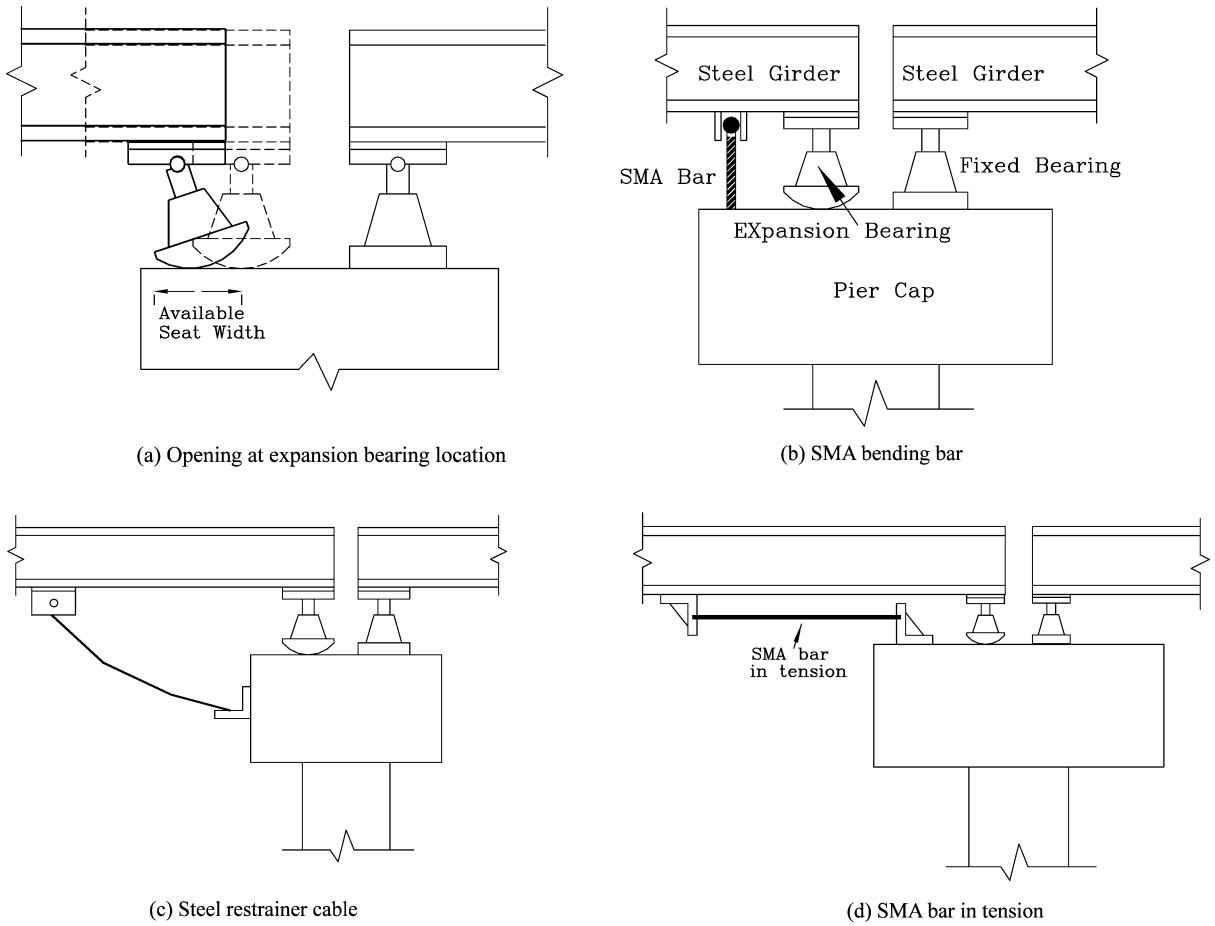

(a) Opening at expansion bearing location

(b) SMA bending bar

(c) Steel restrainer cable

(d) SMA bar in tension

Fig. 13 Available seat-width and installation of the three restrainers

cable was linear up to 30.5 mm and the SMA bending bars were almost linear since the yield strength is very small. However, the tensile SMA bars had bilinear approach up to 30.5 mm and the stiffness hardening beyond that. The three restrainers had the slack of 6.35 mm.

Figure 13 shows the available seat-width of the rocker steel bearings and the installations of the three restrainers. Figure 13(a) shows the movement at the location of expansion bearings. The opening at the location is larger than the available seat-width and, therefore, an unseating occurs. Restrainers can be installed to reduce these openings and prevent the unseating. The installation of the SRCs was placed between deck and cap beam or between deck and abutment at expansion bearing locations. The SMA tensile bars were located at the same places. The two restrainers were placed parallel to the deck and activated only in tension. However, the SMA bending bars were placed perpendicular to the deck and activated in both of backward and forward directions.

6 Deterministic analysis and results

For a nonlinear time history analysis of bridges, ten recorded ground motions shown in Table 1 were used and the nonlinear analysis using them includes various seismic effects. The recorded ground motions, unfortunately, influence the variation in the seismic response of the analysis. In this study, a technique was introduced to manipulate the ten recorded ground motions so that they have the same acceleration response spectrum with expectation to reduce the deviation among the responses. The manipulated ten ground motions were scaled from 0.3 to 0.8 g with an increase

Table 1 List of recorded ground motions

Number	Earthquake	Magnitude	PGA (g)	Station
1	Northridge, 1994, US	6.7	0.617	Beverly Hills
2	San Fernando, 1971, US	6.6	0.324	Castaic-Old Ridge Route
3	Loma Prieta, 1989, US	6.9	0.450	UCSC Link Observatory
4	Mamoth Lakes, 1980, US	6.3	0.430	Long Valley Dam
5	Kobe, 1995, Japan	6.9	0.509	Nishi-Akashi
6	Loma Prieta, 1989, US	6.9	0.329	SF International Airport
7	Chalfant Valley, 1986, US	6.2	0.248	Bishop LADWP-South St.
8	Duzce, 1999, Turkey	7.1	0.535	Duzce
9	Loma Prieta, 1989, US	6.9	0.638	WAHO
10	Inerial Valley, 1979, US	6.5	0.309	Cucapah

of 0.1 g for the nonlinear time history analysis. The mean and standard deviation of the response data were calculated and the values of mean and one standard deviation for each restrainer were compared to evaluate their seismic performance.

Tsai [21] suggested a method to adjust the response spectrum of an acceleration time history in frequency domain using filters and harmonic functions. The method appeared to be a limitation to improve the convergence of the response spectrum. Kaul [22] proposed a technique to adjust the response spectrum in time domain, and the convergence of the spectrum was improved drastically. Lilhanand and Tseng [23] extended the Kaul's method to develop a multi-damping design spectra compatible time history to match multi-damping design spectra. However, the technique did not converge frequently and generated some problems when more than two damping values were tried. Recently, Choi and Lee [24] proposed a procedure to solve the above problems related to the convergence with multi-damping values. This study adopted the method to manipulate the ten time histories and, therefore, they had the same acceleration response spectrum. AASHTO seismic design spectrum [25], which was calculated from the following formulation, was used as the target spectrum in the manipulating process:

$$C_s = \frac{1.2AS}{T^{2/3}} \leq 2.5A \tag{1}$$

where, C_s is the elastic seismic response coefficient, A the acceleration coefficient, S the site coefficient, and T the period of vibration.

In generating the design spectrum, the Soil Profile Type II ($S = 1.2$) was used for the site coefficient since AASHTO recommended it where the soil properties were not known in sufficient detail to determine the soil profile type. The acceleration coefficient, A, is controlled for a specific PGA. Finally, the period, T, can be determined from the condition that C_s is equal to $2.5A$ in (1) and, therefore, the period becomes 0.437 seconds.

Figure 14(a) shows the response spectra of the ten ground motions scaled to 1.0 g PGA and their average spectrum which is compared to the target spectrum. As shown in Fig. 14(a), the target spectrum is amplified compared to the average one after the period of 0.3 seconds and the maximal pseudo-acceleration of the target spectrum is 2.542 g which is a little less than the maximum of 2.6347 g for the average spectrum. Figure 14, (b) and (c), compares the spectra and the time histories of the original and the manipulated ground motions of Northridge earthquake, 1994.

An SRC, an SMA-T bar, or one set of 20 SMA-B bars was installed for each girder at the location of expansion bearings. The effective stiffness of the restrainers was respectively 62.7, 49.3, and 50.6 kN/mm for SRC, SMA-T, and SMA-B. Also, the initial stiffness of the SMA-T restrainer was 141.1 kN/mm. The suite of the ten manipulated ground motions was scaled from 0.3 to 0.8 g to respectively represent the moderate and strong earthquakes; the PGA of 0.3, 0.4, and 0.5 g represents the moderate ground shakes and that of 0.6, 0.7, and 0.8 g the strong ones. The interesting responses are column drift ratio, opening at expansion bearings, and the abutment deformations in active and passive actions; these are influenced largely by the restrainers installed. The mean and one standard deviation of the ten responses for each PGA level are plotted in Fig. 15.

Fig. 14 Manipulation of acceleration time history

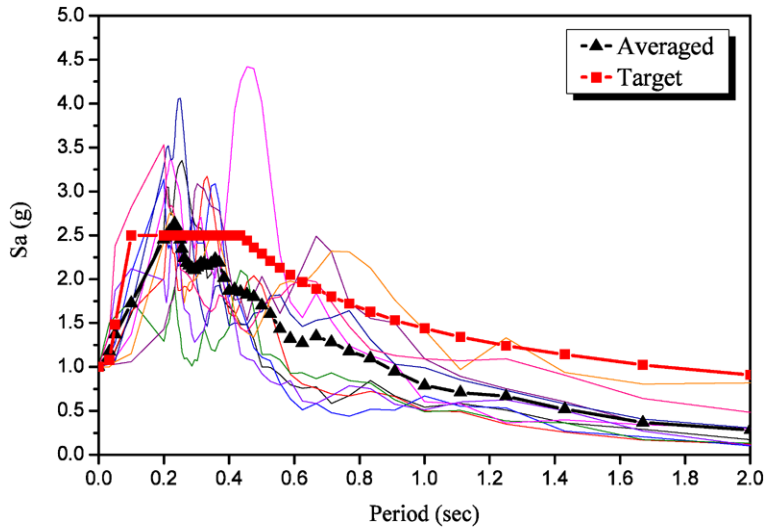

(a) Response spectra of 10 ground motions and target spectrum

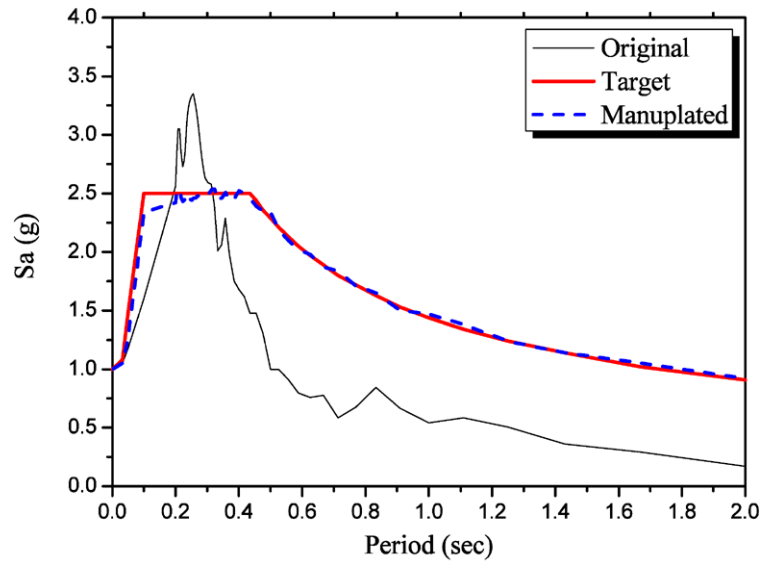

(b) Comparison of the response spectra between the original and the manipulated ground motion

The three restrainers reduced the drift ratios of the columns as shown in Fig. 15, (a) and (b); the drift ratio describes the top displacement of the pier divided by the pier length. In the column 'Col1', the three types of restrainers showed almost the same and satisfactory response. The reduction rates, for the SMA-B type, were 32.6 and 11.0% for 0.3 and 0.8 g, respectively. Thus, the effect of the restrainers for the 'Col1' was reduced by increasing the PGA of the ground motions. For 'Col2', on the contrary, the restrainers showed better results against strong ground motions. The reduction rates, for the SMA-T type, were 12.0 and 32.8% for 0.3 and 0.8 g, respectively. The SMA-T and the SRC produced almost the same drift ratios for 'Col2'. However, the SMA-B showed better results than the other two types for the moderate ground motions of 0.3, 0.4, and 0.5 g PGA but worse results for the strong ground motions of 0.6, 0.7, and 0.8 g PGA.

Fig. 14 (*Continued*)

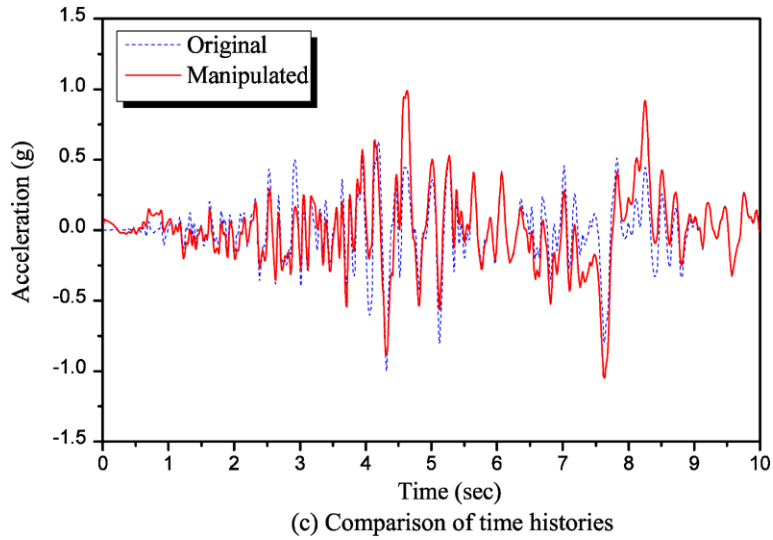

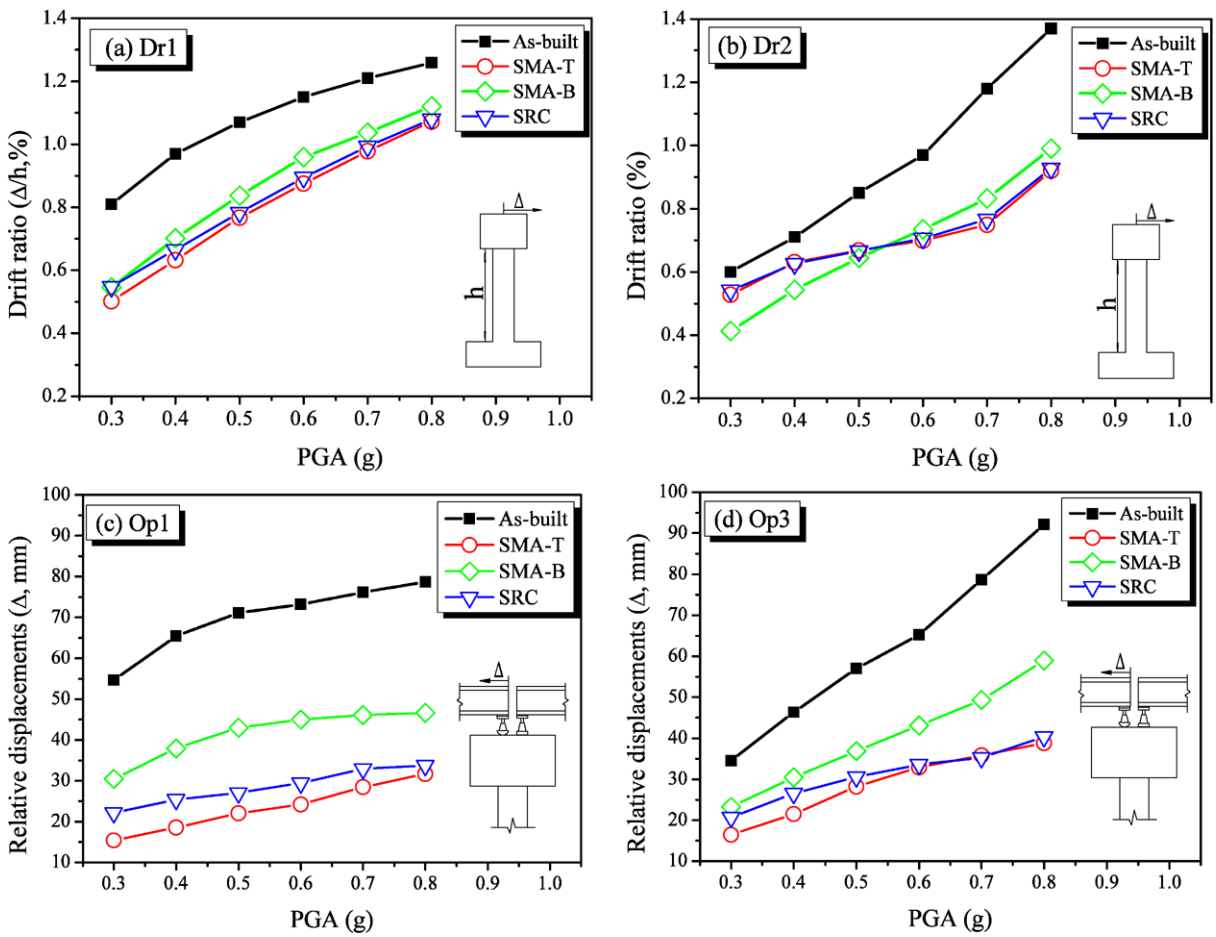

Fig. 15 Envelope of the interesting responses; Dr: drift ratio, Op: opening, Ab-a: abutment displacement in active action, Ab-p: abutment displacement in passive action

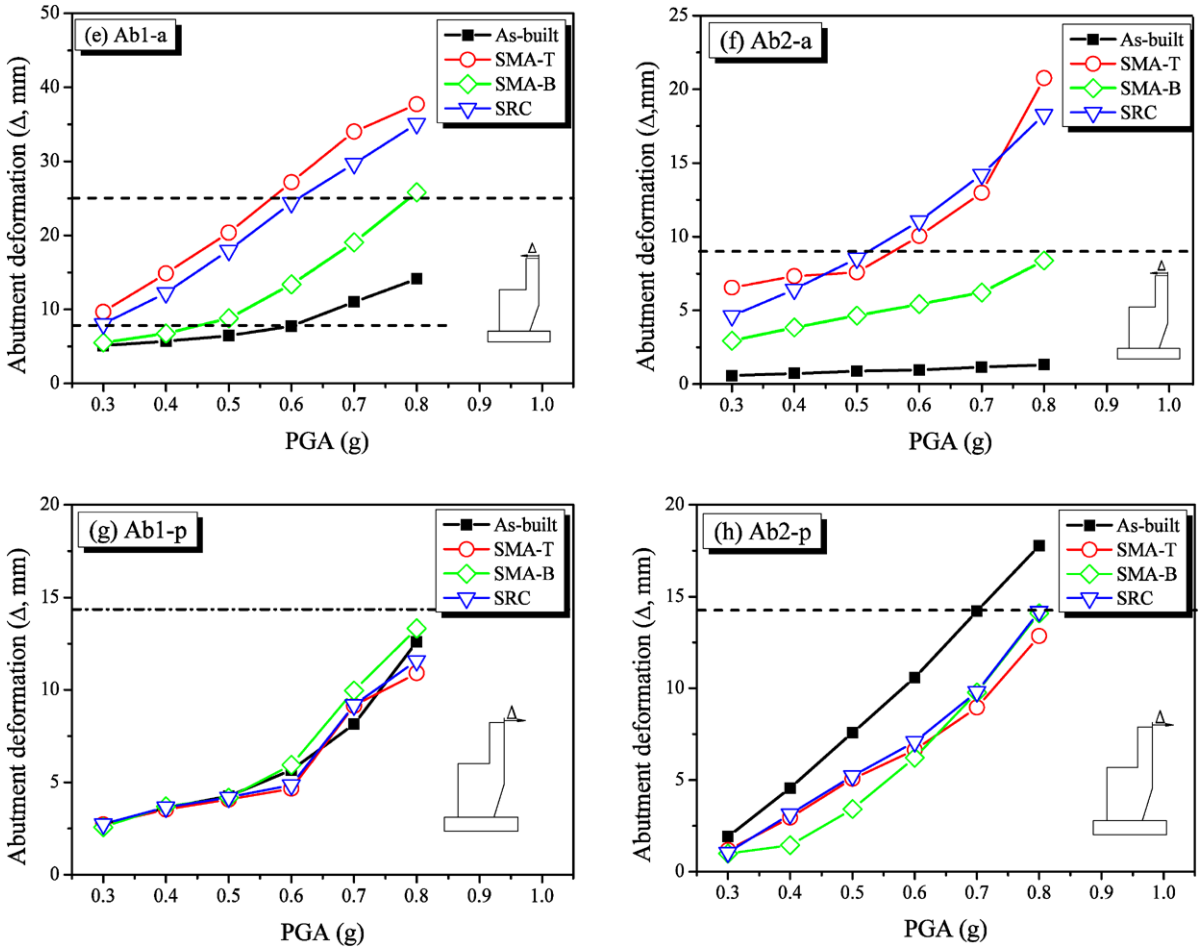

Fig. 15 (*Continued*)

In Fig. 8, the maximum opening was generally developed at 'Op1' or 'Op3'. 'Op2' is much lesser than the other two since the two piers moved in phase motion. Thus, 'Op2' will not be discussed. The SMA-T was the most effective among the three types and reduced the maximum opening from 78.75 and 92.13 mm to 31.68 and 38.85 mm at 'Op1' and 'Op3', respectively, with 0.8 g PGA. Although the worst effective type was the SMA-B, it reduces the maximum opening to 46.65 mm and 57.80 mm at 'Op1' and 'Op3', respectively, with 0.8 g PGA; which was a satisfactory result. The result of the SRC was similar to that of the SMA-T. Therefore, the three types of restrainers were effective in preventing the unseating in the MSSS bridges.

For the abutments, the three restrainers increased abutment active deformation largely, especially on 'Ab2', having expansion bearings on it. The dot lines on the graphs represent the first yield (7.4 mm) and the ultimate deformation (25.4 mm), respectively. With employing the restrainers, the abutment active deformations were beyond the first yield point and reached the ultimate deformation at 'Ab1' due to the strong ground shakes. Among the three, the worst restrainer was the SMA-T which generated the active deformation over the first yield even with the 0.3 g PGA ground motion. The SRC and the SMA-T restrainers reached the ultimate deformation (25.4 mm) even at the 0.6 g PGA, which means the two types cannot be used without a reinforcement on the abutment for strong ground shakes. However, the SMA-B controlled the active deformations under the first yield point with the moderate ground shakes of 0.3 and 0.4 g at 'Ab1' and generated the 25.8 mm active de-

formation just at the 0.8 g. For 'Ab2', it also protected the abutment from the first yield damage. Although the SMA-T restrainer reduced the opening most effectively, it transferred large force to the abutments in active action and generated large deformation on them.

The passive deformation of abutments in bridges is generally governed by the pounding from decks. Thus, for 'Ab1', the restrainers did not reduce the pounding forces and produced almost the same responses as the as-built bridge. For 'Ab2', they showed the effectiveness to reduce the passive deformation. Especially, the SMA-B reduced the passive deformation from 4.56 and 7.58 mm to 1.45 and 3.42 mm against 0.4 and 0.5 g, respectively, and the reduction rates were 68.2 and 54.9%. The SMA-B was so much activated in closing that it resisted the deck's closing movement to 'Ab2'. The action of the SMA-B, different from the other two, was beneficial to reduce the passive deformation against the moderate ground shakes.

The restrainers installed at each girder reduced drift ratios moderately and openings effectively. However, the restrainers increased the active abutment deformation and produced the first yield even with the moderate ground motions of 0.3, 0.4 and 0.5 g, except for the SMA-B restrainer. For the passive action of the abutment, only the SMA-B restrainer was effective moderately to control the pounding on the abutments. On the whole, the SMA-T restrainer was the most effective to reduce openings but the worst on the active deformation of abutments. The SMA-B was very good at the active deformation of abutments even with strong ground motions. However, the SMA-B was the worst to reduce openings.

From the deterministic analysis, it is understood how the three restrainers influenced each component. However, it cannot be determined which restrainer is the most effective for the whole bridge system.

7 Fragility analysis and results

A fragility analysis can assess the performance of each bridge component probabilistically and combine the assessment of each component for a whole bridge system. Therefore, the employment of a fragility analysis can overcome the weakness of the above deterministic analysis. A fragility curve represents the probability of reaching or exceeding a damage state as a function of ground motion intensity parameter, such as peak ground acceleration. The probability of failure (P_f), which means that the demand on the structure exceeds the structural capacity, can be described by (2):

$$p_f = P\left[\frac{S_d}{S_c} \geq 1\right] \tag{2}$$

where P_f is the probability of exceeding a specific damage state, S_d is the structural demand and S_c the structural capacity.

In general, the probability is described as lognormal distribution because it has shown to be a good fit in the past [26]. In this case, the structural capacity and seismic demand are also described by a lognormal distribution. Thus, the fragility curve can be represented by a lognormal cumulative distribution function as follows:

$$P_f = \Phi\left[\frac{\ln(S_d/S_c)}{\beta}\right] \tag{3}$$

where β is logarithmic standard deviation known as the dispersion, and $\Phi[\cdot]$ is the standard normal distribution function.

The fragility curves for each component are calculated using probabilistic seismic demand models based on (3). Table 2 illustrates the damage states for the components used in (3). The definition of the damage states for column drift ratios are based on Duta's study [27]. The definitions of damage states for other three components are from Choi's study [19]. The fragility curves for the whole bridge system can be obtained from (4):

$$P(F_{\text{sys}}) = 1 - \prod_{i=1}^{m}\left[1 - P(F_i)\right] \tag{4}$$

where, $P(F_{\text{sys}})$ is the probability of failure for the overall bridge system and $P(F_i)$ the probability of failure for each component.

This study followed the same procedure as Choi's study [19] to obtain the fragility curves of bridge components and the bridge system; to save the space, the authors will not repeat it here.

The four components considered in this analysis had several subcomponents (columns 1 and 2, abutments 1 and 2, etc.). Thus, the most vulnerable subcomponent was used to represent the fragility of the component. For example, 'Col1' was the most vulnerable one for the columns and 'Ab1' in active and passive action was the most vulnerable one for the

Table 2 Definition of damage states for bridge components

Damage State	No Damage	Slight Damage	Moderate Damage	Extensive Damage	Complete Damage
Columns (dr, %)	$dr \leq 0.5$	$0.5 < dr \leq 0.7$	$0.7 < dr \leq 1.5$	$1.5 < dr \leq 2.5$	$2.5 \leq dr$
Openings (δ, mm)	$\delta \leq 50$	$50 < \delta \leq 100$	$100 < \delta \leq 150$	$150 < \delta \leq 255$	$255 \leq \delta$
Abutments in Active Action (δ, mm)	$\delta \leq 4$	$4 < \delta \leq 8$	$8 < \delta \leq 25$	$25 < \delta \leq 50$	$50 \leq \delta$
Abutments in Passive Action (δ, mm)	$\delta \leq 7$	$7 < \delta \leq 15$	$15 < \delta \leq 37$	$37 < \delta \leq 146$	$146 \leq \delta$

abutments. In the fragility curves, the median value is the PGA corresponding to 50% of the probability of exceeding a damage-state. In this section, the author wanted to use the median values of the fragility curves as the indicator of the seismic resistance of the components: the component showing a larger median value for a specific damage-state has more seismic resistance against the damage-state.

The median values of the slight and the moderate damage states were estimated and shown in Fig. 16. Figure 16(a) for the slight damage state indicates that the median values of column drift ratio, opening, and abutment passive deformation increased by the restrainers compared to those of the as-built bridge. Among the three restrainers, the SMA-B enlarged the seismic resistance of the three components most effectively; the increments of the SMA-B for the column, the opening, and the abutment passive deformation were 55.2, 140.7, and 49.0%, respectively. The median value of the slight damage state for the abutment active deformation of the as-built bridge was 0.355 g. The median values of the SRC, the SMA-T, and the SMA-B restrainers were 0.210, 0.188, and 0.22 g, respectively. Thus, the three restrainers increased the seismic vulnerability of the abutment in active action. However, the SMA-B restrainer increased the vulnerability by 37.5%, which was less than 40.8% of the SRC and 47.0% of the SMA-T restrainer. For the moderate damage state from Fig. 16(b), the overall trend was similar to that of the slight damage state. Therefore, it can be said based on the review of the fragility curves of the components that the SMA-B restrainer was the most effective to increase the seismic resistance of the column, the opening, and the abutment passive deformation. Also, although the three restrainers decreased the seismic resistance of the abutment in active action, the SMA-B restrainer showed the smallest decrement.

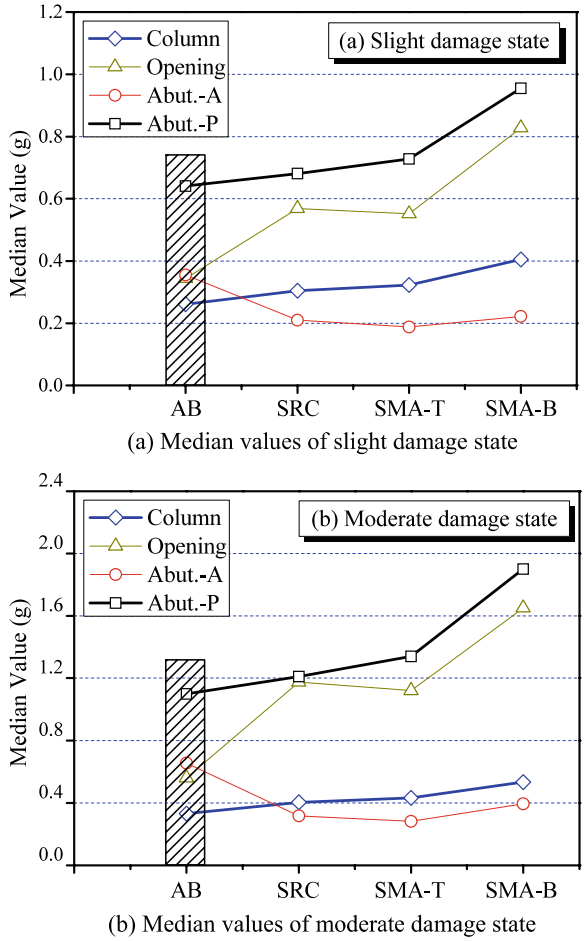

Fig. 16 Comparison of median values for the four bridge types

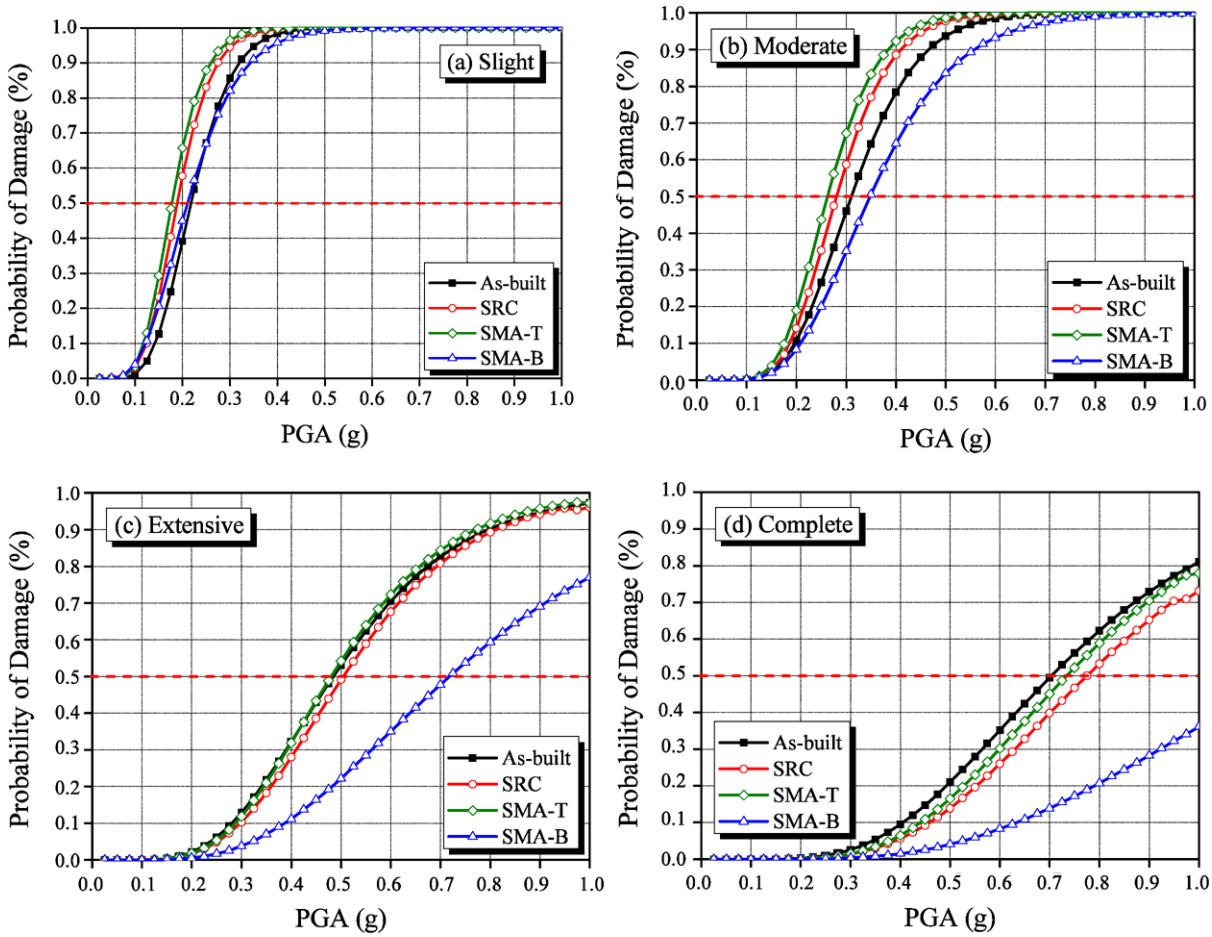

Fig. 17 Fragility curves for the as-built and the three retrofitted bridges

Figure 17 shows the bridge-system fragility curves for the as-built and the three types of retrofitted bridges. As in the fragility curves of the components, the median values of the combined fragility curves indicate the seismic resistance of the whole bridge system. Figure 18 shows the median values of the four damage states for the as-built and the retrofitted bridges.

The median values for the as-built bridge are 0.218, 0.310, 0.483 and 0.705 g for all the damage-states. The SMA-B restrainer decreased a little the median value by 3.7% for the slight damage state. However, the SMA-B restrainer showed a larger median value by 12.3% for the moderate damage state than that of the as-built bridge. Also, the median values of the SMA-B restrainer for the extensive and complete damage states were larger by 48.9% and 70.2%, respectively, comparing to those of the as-built bridge. Therefore,

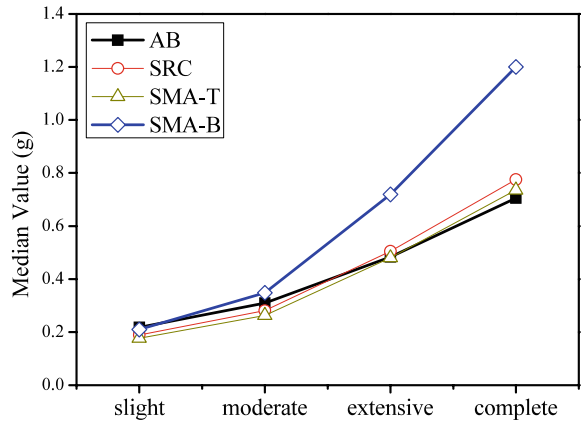

Fig. 18 Median values of all damage states for the four types of bridges

the SMA-B restrainer effectively increased the seismic resistance of the bridge for the serious damage states which were related to moderate or strong ground shakings. Also, it can be stated certainly that the SMA-B restrainer showed the effectiveness to reduce the seismic vulnerability of the MSSS bridge.

For the SRC restrainer, the median values for slight and moderate damage states were less than those of the as-built bridge. The restrainer increased the seismic vulnerability of the bridge for extensive and complete damage states by 4.6 and 9.9%. The SMA-T restrainer produced smaller median values for the first three damage states than those of the as-built bridge. It increased the seismic resistance only for complete damage state. The two types of restrainers, SRC and SMA-T, sacrificed the abutment to reduce the column drift ratio and the opening. Since the abutments were more vulnerable in active action than in passive action, the SRC and the SMA-T restrainers, which transferred the developed seismic force only to the abutments in active action, did not improve effectively the seismic resistance of the overall bridge system. Conversely, the SMA-B restrainer delivered the seismic force both in active and passive actions of the abutment, thus reducing the damage probability on the abutment in active action.

8 Conclusions

The three types of restrainers, such as SMA bars in tension and bending and steel restrainer cables, were assessed for the seismic performance of the multi-span-simply-supported (MSSS) bridge. From the deterministic analysis, all the restrainers reduced the column drift ratios and the openings at the expansion bearing locations effectively. However, they produced the yield of abutments in active action. The SMA bars in tension were the most effective to control the openings but the worst on the active deformation of abutments since they had large initial stiffness compared to the other two restrainers and the hardening beyond the deformation of 30.2 mm.

The abutment with fixed bearings was more vulnerable than the abutment with the expansion bearings when the restrainers were installed on it. Only the restrainer of the SMA bending bars retained the abutment with fixed bearings below the first yield deformation against moderate ground shakes of 0.3, 0.4, and 0.5 g. Also, the SMA bending bars prevented the pounding on the abutment 'Ab2' against the moderate ground motions although the other two restrainers permitted the pounding at the moderate ground motions. The deterministic analysis indicated that the steel restrainer cables and the SMA bars in tension were more effective to reduce the openings than the SMA bars in bending. However, the two restrainers sacrificed the abutment in active action more than the SMA bars in bending. The deterministic analysis showed how each restrainer acted on the components of the bridge but could not estimate the restrainers' effect on the whole bridge system.

The fragility analysis showed the influence of the restrainers on the bridge system using the combination of the fragility curves of the components. The fragility analysis maintained that the SMA bars in bending were the most effective in increasing the seismic resistance of the bridge. The other two restrainers cannot be estimated as effective restrainers. They decreased the seismic resistance for the slight and the moderate damage states and just increased it slightly for the extensive and the complete damage states. This result interpreted that the steel restrainer cables and the SMA bars in tension should be used with caution for the MSSS bridges.

Considering all the above results, the restrainer of the SMA bending bars was the most appropriate for the MSSS bridges to control openings without the damage on abutments in active action against moderate ground motions. Also, as Dicleli [28] mentioned, the SMA bending bars in seismically isolated bridges can provide supplemental elastic stiffness and reduce displacements in isolation-devices.

Acknowledgements This study has been supported by the Basic Science Research Program through the National Research Foundation of Korea funded by the Ministry of Education, Science and Technology (Project No. 2009-0087163). The authors would like to acknowledge the financial support.

References

1. Copper, J.D., Friedland, I.M., Buckle, I.G., Nimis, R.B., Bob, N.M.: The Northridge Earthquake: progress made, lessons learned in seismic-resistant bridge design. Public Roads **58**, 26–36 (1994)
2. CALTRANS: Bridge Design Specifications Manual. California Department of Transportation (1990)
3. DesRoches, R., Delemont, M.: Seismic retrofit of simply supported bridges using shape memory alloys. Eng. Struct. **24**, 325–332 (2002)

4. Dolce, M., Cardone, D., Marnetto, R.: Implementation and testing of passive control devices based on shape memory alloys. Earthq. Eng. Struct. Dyn. **29**, 945–968 (2000)
5. Wilde, K., Gardoni, P., Fukino, Y.: Base isolation system with shape memory alloy device for elevated highway bridges. Eng. Struct. **22**, 222–229 (2000)
6. DesRoches, R., McCormick, J., Delemont, M.: Cyclic properties of superelastic shape memory alloy wires and bars. ASCE J. Struct. Eng. **130**(1), 38–46 (2004)
7. Andrawes, R., DesRoches, R.: Unseating prevention for multiple frame bridges using superelastic devices. Smart Mater. Struct. **14**, s60–s67 (2005)
8. Ocel, J., DesRoches, R., Leon, R.T., Hess, W.G., Krumme, R., Hayes, J.R., Sweeney, S.: Steel beam column connections using shape memory alloys. ASCE J. Struct. Eng. **130**(5), 732–740 (2004)
9. Adachi, Y., Unjoh, S., Kondoh, M.: Development of a shape memory alloy damper for intelligent bridge systems. In: Proceedings of the International Symposium on Shape Memory Materials, Kanazawa, Japan, pp. 31–34 (1998)
10. Choi, E., Lee, D.H., Choei, N.-Y.: Shape memory alloy bending bars as seismic restrainers for bridges in seismic areas. Int. J. Steel Struct. **9**(4), 261–273 (2009)
11. Duerig, T., Pelton, A., Stockel, D.: An overview of nitinol medical applications. Mater. Sci. Eng. A **273–275**, 149–160 (1999)
12. Kaounides, L.: Advanced materials—Corporate strategies for competitive advantage in the 1990s. FT Management Reports, Pearson Professional Ltd., London (1995)
13. Tobushi, H., Hashimoto, T., Shimeno, Y., Takata, K.: Fatigue properties of TiNi shape memory alloy. Mater. Sci. Forum **327–328**, 151–154 (2000)
14. Wagner, M., Sawaguchi, T., Kaustrater, G., Hoffken, D., Eggeler, G.: Structural fatigue of pseudoelastic NiTi shape memory wires. Mater. Sci. Eng. A **378**, 105–109 (2004)
15. Miyazaki, S., Mizukoshi, K., Ueki, T., Sakuma, T., Liu, Y.: Fatigue life Ti-50 at.% Ni and Ti-40Ni-10Cu (at.%) shape memory alloy wires. Mater. Sci. Eng. A **273–275**, 658–663 (1999)
16. Johnson, R., Padgett, J.E., Maragakis, M.E., DesRoches, R., Saiidi, S.: Large scale testing of nitinol shape memory alloy devices for retrofitting of bridges. Smart Mater. Struct. **17**, 1–10 (2008)
17. Prakash, V., Powell, G.H., Campbell, S.D., Filippou, F.C.: DRAIN 2DX User Guide. Department of Civil Engineering, University of California at Berkeley (1992)
18. Mander, J.B., Kim, D.K., Chen, S.S., Premus, G.J.: Response of steel bridge bearings to the reversed cyclic loading. Technical Report NCEER 96-0014, Buffalo, NY (1996)
19. Choi, E., DesRoches, R., Nielson, B.: Seismic fragility of typical bridges in moderate seismic zones. Eng. Struct. **26**, 187–199 (2004)
20. Maroney, B., Karl, R., Kutter, B.: Experimental testing of laterally loaded large scale bridge abutments. In: Structural Engineering in Natural Hazards Mitigation, pp. 1065–1070 (1993)
21. Tsai, N.C.: Spectrum-compatible motions for design purposes. ASCE J. Eng. Mech. Div. **98**, 345–356 (1972)
22. Kaul, M.K.: Spectrum-consistent time-history generation. ASCE J. Eng. Mech. Div. **104**, 781–788 (1978)
23. Lilhanand, K., Tseng, W.S.: Generation of synthetic time histories compatible with multiple damping design response spectra. In: SMiRT-9, Lausanne, Switzerland, K2/10, pp. 105–110 (1987)
24. Choi, D.H., Lee, S.H.: Multi-damping earthquake design spectra compatible motion histories. Nucl. Eng. Des. **226**, 221–230 (2003)
25. AASHTO: AASHTO LRFD Bridge Design Specifications, SI Units 4th Edition. American Association of State Highway and Transportation Officials, Washington, DC (2007)
26. Wen, Y.K., Wu, C.L.: Uniform hazard ground motions for Mid-America cities. Earthq. Spectra **17**(2), 359–384 (2001)
27. Dutta, A., Mander, J.B.: Seismic fragility analysis of highway bridges. In: Proceedings of the Center-to-Center Project Workshop on Earthquake Engineering in Transportation System, Tokyo, Japan (1999)
28. Dicleli, M.: Supplemental elastic stiffness to reduce isolator displacement for seismic-isolated bridges in near-fault zones. Eng. Struct. **29**, 763–775 (2007)